

Two-dimensional turning of thermal flux from normal to lateral propagation in thin metal film irradiated by femtosecond laser pulse

V V Shepelev¹ and N A Inogamov^{2,3}

¹ Institute for Computer-Aided Design of the Russian Academy of Sciences, Vtoraya Brestskaya 19/18, Moscow 123056, Russia

² Landau Institute for Theoretical Physics of the Russian Academy of Sciences, Akademika Semenova 1a, Chernogolovka, Moscow Region 142432, Russia

³ Dukhov Research Institute of Automatics (VNIIA), Sushchevskaya 22, Moscow 127055, Russia

E-mail: vadim.v.shepelev@gmail.com

Abstract. There are various geometrical variants of laser illumination and target design. Important direction of investigations is connected with tightly focused action (spot size may be less than micron) onto a thin metal film: thickness of a film is just few skin-layer depths. Duration of a pulse is $\tau_L \sim 0.1$ ps. In these conditions energy absorbed in a skin layer first propagates normally to a surface: gradient $\partial T_e / \partial x$ dominates, here and below x and y are normal and lateral directions. This process in 1–2 ps homogenizes electron temperature T_e along thickness of a film. We consider conditions when a film or is supported by weakly conducting substrate, or is free standing. Therefore all absorbed energy is confined inside the film. At the next stage the internal energy begin to flow along the lateral direction—thus direction of energy expansion is changed from x to y because of the heat non-penetrating boundary condition imposed on the rear-side of the film. At the short two-temperature stage of lateral expansion the thermal conductivity κ is high. After that electron and ion temperatures equilibrates and later on the heat propagates with usual value of κ . Lateral expansion cools down the hot spot on long time scales and finally the molten spot recrystallizes. Two-dimensional approach allows us to consider all these stages from propagation in x direction (normal to a film) to propagation in y direction (along a film).

1. Introduction

There are many technological applications (from plasmonics to medicine) where diffraction limited focal spot is applied onto a thin film, see important examples listed in [1–7]. Thickness of these thin films is $d_f \approx 50$ nm. For optical lasers the depth of the skin layer in metal is $\delta_{sk} = 10$ –20 nm. Experimental films often are made from gold or silver, but sometimes other metals are used (copper [8], nickel [9], or multilayer elastic films for flexible electronics [10]). Below we consider example corresponding to some typical metal. We study process of thermal redistribution of absorbed laser energy from a skin layer of an illuminated spot along film thickness and lateral directions of a planar film (figure 1). The film melts as result of absorption heating and after that cools and recrystallizes.

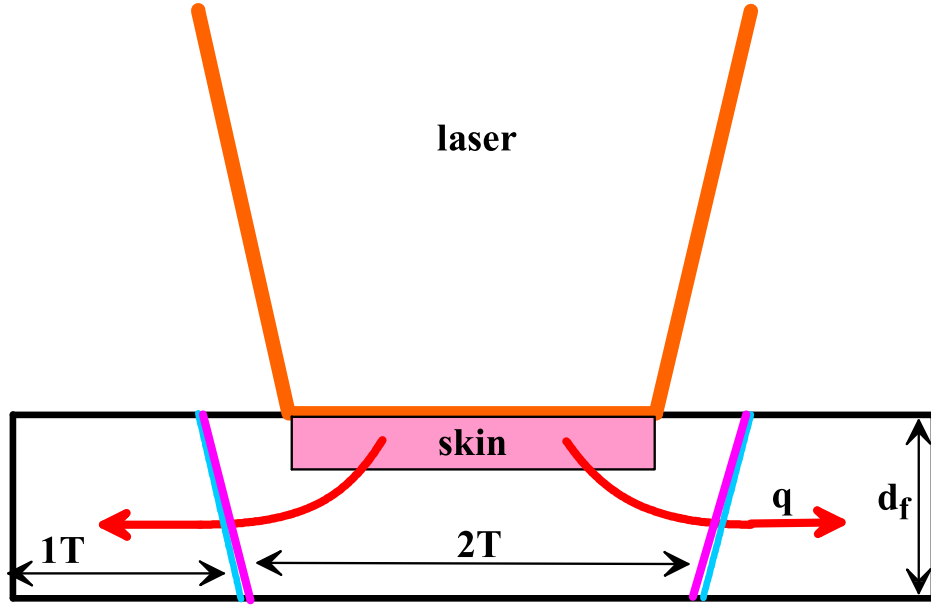


Figure 1. Scheme of action of an ultrashort laser pulse onto a thin film. Energy is absorbed in a skin layer which is thinner than depth of a film: $\delta_{\text{sk}} = 15$ nm, $d_f = 50$ nm, $\tau_L = 100$ fs in the simulation presented below. Lateral size of a beam on the frontal surface of a beam is $2R_L$ —this is diameter of a focal spot. The scheme shows transitions from 2T to 1T stage together with the turn: 1D–2D–1D, where the first 1D relates to propagation from the skin along the direction x normal to a film, the “2D” in the chain 1D–2D–1D is the turn taking place during the 2T–1T transition, and the last “1D” in the chain stands for 1T lateral expansion of absorbed energy along the y -direction. This expansion cools the hot spot which is solidified at the subnanosecond time scale.

2. General picture

Even the smallest spot, few 100s nm in diameter $2R_L$, may be approximately described in 1D approximation because still its thickness is small relative to diameter: $d_f/R_L \ll 1$. Usually the two-temperature (2T) stage is numerically simulated in 1D approximation with one-dimensional two-temperature hydrodynamic (1D–2T–HD) code [11–14]. While the subsequent lateral expansion of heat is described analytically. Analytic approach is done or supposing constant thermal conductivity coefficient κ corresponding to the one-temperature (1T) conditions, or with inclusion of the short 2T stage when we have strongly enhanced values of κ [5, 15].

Qualitatively figure 1 shows the main processes discussed below:

- (i) illumination by laser beam of a focal spot with lateral size $2R_L$ on surface of a film;
- (ii) absorption of energy and heating of electron subsystem inside the skin circle $2R_L$; the heating follows the intensity distribution of the beam along the frontal surface;
- (iii) fast (at the one picosecond time scale) expansion (previously called ballistic transport) of absorbed energy in direction of the axis x ; thus the electron temperature distribution $T_e(x, y, t)$ becomes homogeneous along the x -direction: $T_e(x, y, t) \rightarrow T_e(y, t)$; but this distribution is inhomogeneous in the y -direction;
- (iv) there is the geometrical turn from the mainly normal direction (x -direction) of heat flux to the mainly lateral direction (y -direction) of heat flux. The turn is shown in figure 1. The q_x component of heat flux is large at the early stage when heat propagates mainly in normal direction and q_x dominates over lateral flux q_y . The q_x component is large because

gradient of electron temperature is large $\sim 10^{12}$ K/m at this stage. After that the gradient $(T_e)_x$ sharply drops down (T_e becomes homogeneous along the x -axis) and the turn of heat flux takes place. Later in time the q_y component dominates over the q_x component. Due to difference in the spatial scales the lateral q_y is much less than the maximum value of the normal flux q_x at the early stage;

- (v) finally the 1T lateral q_y cooling drops down the temperatures in the molten central circle $2R_L$ and metal solidifies.

3. Equations

In the paper below we will not use simplifying assumptions $d_f/R_L \ll 1$ or approximate analytic descriptions. We apply 2T thermal equations in two dimensions (2D) and solve them numerically by the finite differences algorithm (2T–2D approach). In one-dimensional (1D) geometry (2T–1D approach) these equations were firstly proposed in the important paper written by Anisimov, Kapeliovich, and Perel'man in 1974 year [16], far before the era of wide using of lasers with ultrashort pulses begins. Recently 2T–2D approach was applied to investigations of effect of periodic surface modulation of laser intensity along absorbing boundary to T_e and after that to T_i evolutions of the temperature fields [17]. Here we consider the T_e, T_i evolutions driven by illumination of a solitary laser spot.

2T, 2D system of equations is

$$\rho \frac{\partial(E_e/\rho)}{\partial t} = \nabla q - \alpha (T_e - T_i) + P; \quad q = -\kappa \nabla T_e; \quad (1)$$

$$\rho \frac{\partial(E_i/\rho)}{\partial t} = \alpha (T_e - T_i). \quad (2)$$

This system follows from 1T energy equation when we split energy budgets for electron subsystem (1) and ion subsystem (2). Here E_e, E_i are internal energies of electrons and ions per unit of volume, a vector q is an electron heat flux, coefficient α defines the rate of energy exchange between electron and ion subsystems. The coefficient α is called electron-ion coupling parameter. We take the coefficients α and κ according to papers [18–21] for different metals. Figures 2–4 show results of simulation for $\alpha = 10^{17}$ W/K/m³ and κ typical for Al and Au.

In our simulations we neglect motion of matter. Motion of a film of course takes place [5–7] but it does not change qualitatively picture of cooling up to freezing if formation of a jet and rupture of a film are absent. Motion changes area and thickness of a film in a central region thus influencing cooling process. As is said below, we use 2T–2D approach to answer to two questions. First of them is how much a heated spot enlarges in its lateral size during 2T stage. This is important because delamination of a film from substrate takes place shortly after 2T stage, and lateral size of delaminated area is defined by the size of a heated spot at the stage of delamination. The second question is devoted to a recrystallization process. 2T stage lasts few picoseconds while motion proceeds with velocities of the order of 10s m/s. Therefore we can neglect influence of motion to the answer on the first question. But formation of a jet and rupture of a film changes quantitatively an answer to the second question. But the qualitative picture remains as it is described here.

We use equation of state (EoS) for Al in our simulations; it is taken from works [11, 12, 22–26]. Heating and cooling proceed isochorically because we neglect motion. This influences melting temperature increasing it from the value in a triple point. Using EoS allows us to include latent heat of melting (heat of fusion) while in other papers using 2T equations, authors say that solid is melt as its temperature achieves melting temperature and ignore heat of fusion.

The source P in electron energy equation (1) in 1D is

$$P(x, t) = F_{\text{abs}} / (\sqrt{\pi} \tau_L \delta_{\text{sk}}) \exp(-x/\delta_{\text{sk}}) \exp(-t^2/\tau_L^2).$$

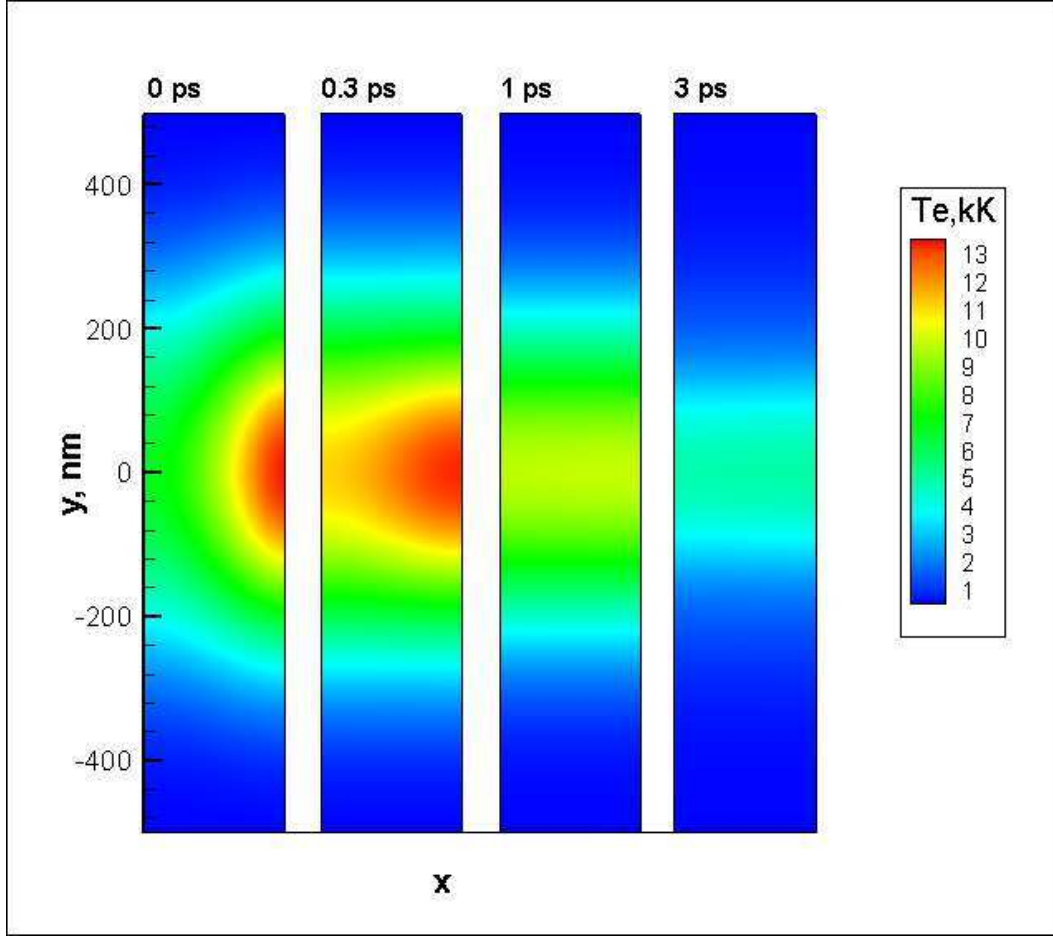


Figure 2. Evolution of the electron temperature field $T_e(x, y, t)$. The frames for $t = 0$ and 0.3 ps shows expansion of absorbed heat from the skin-layer $\delta_{sk} = 15$ nm along the x -direction. This expansion and the thermally isolated rear-side boundary (opposite to the illuminated side) very soon lead to equalization of T_e along thickness of a film: $T_e(x, y, t) \rightarrow T_e(y, t)$, see the last two frames. Aspect ratio of the rectangular box (corresponding to the simulated film) is 1000 nm : 50 nm = 20 : 1. We impose boundary conditions $\partial T_e(x = 0, -50; y, t)/\partial x = 0$, $T_e(x, y = \pm L_{box}, t) = 0.3$ kK. Thickness of a heat affected zone (HAZ) is significantly more than thickness 50 nm of our film. Therefore the component $(T_e)_x$ of a gradient quickly strongly decreases under illuminated laser spot.

Surface density of absorbed energy F_{abs} [mJ/cm²] here is homogeneous along the irradiated vacuum boundary of a film. Equally well the same irradiation may come through transparent substrate and be absorbed in the skin near the contact boundary.

In 2D the energy source is

$$P(x, y, t) = \frac{F_{abs}}{\sqrt{\pi} \tau_L \delta_{sk}} \left[\exp\left(-\frac{y^2}{R_L^2}\right) - \exp\left(-\frac{R_{box}^2}{R_L^2}\right) \right] \exp\left(-\frac{x}{\delta_{sk}}\right) \exp\left(-\frac{t^2}{\tau_L^2}\right). \quad (3)$$

The distribution (3) corresponds to illumination by a cylindrical lens. The lens produces an illuminated straight line directed normally to the plane x - y . Maximum fluence is achieved in the point $y = 0$. Value $F_{abs}[1 - \exp(-R_{box}^2/R_L^2)]$ corresponds to this maximum. In simulation below we take $L_{box} = 500$ nm and $R_L = 180$ or 90 nm. The small term $\exp(-R_{box}^2/R_L^2) = 4 \times 10^{-4}$ is

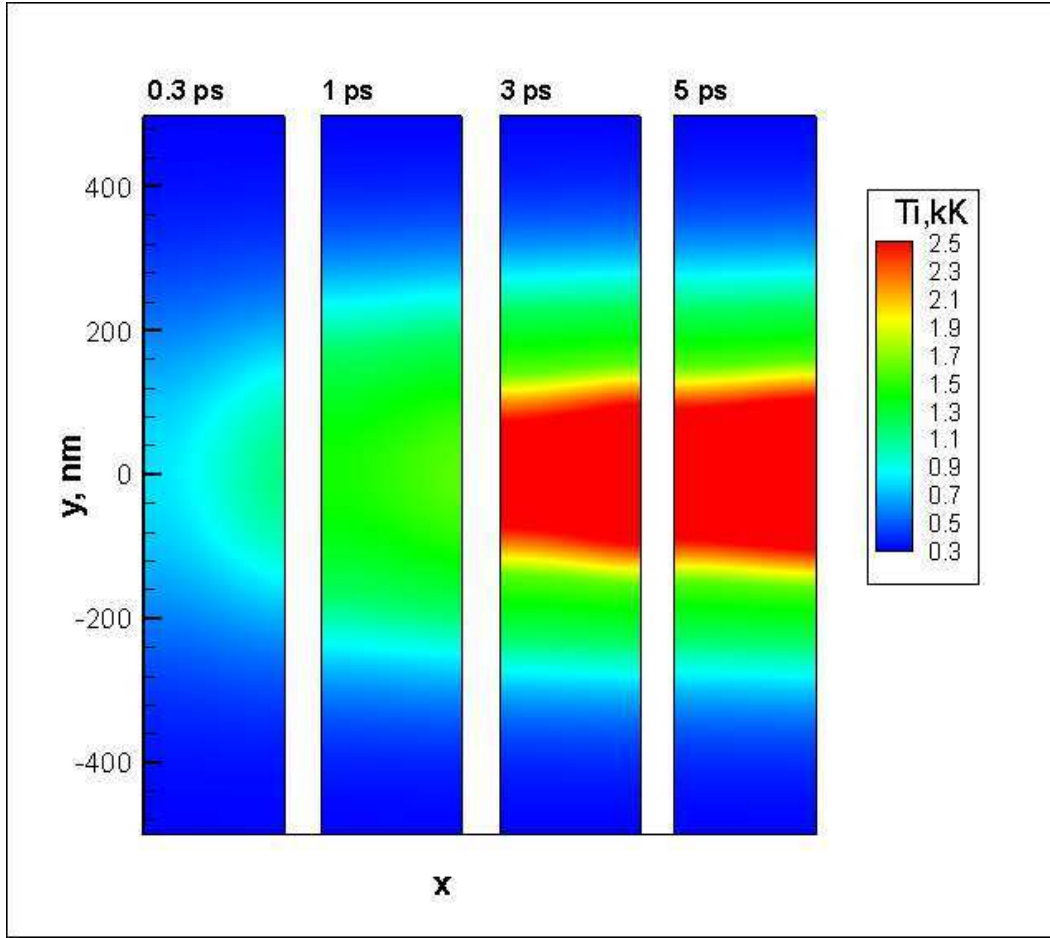


Figure 3. Evolution of the ion temperature field $T_i(x, y, t)$. First, the ions get energy from electrons at the early stage following the expansion of T_e in the direction to the rear-side: $t = 0.3$ ps. After that the ion temperatures also become mainly distributed laterally. Their lateral distribution slowly spreads out.

necessary to correct absorbed power at the edge point. With this correction the volume power (3) is zero at the edges $y = \pm L_{\text{box}}$ of a rectangular simulation box. The box occupies rectangular $-d_f < x < 0$, $-L_{\text{box}} < y < L_{\text{box}}$; as was said $d_f = 50$ nm. Below we present results for absorbed energies F_{abs} varying from 10 to 100 mJ/cm². For the simulation given below we choose the plane geometry (3); it corresponds to action of laser through a cylindrical lens.

4. Two problems

In the paper we shed light on the two problems (I) and (II).

(I) First, can the 2T thermal flux enlarge the lateral size of the hot spot beyond the optical diameter $2R_L$ prior to the stage of separation of a film from substrate? If yes than the separation diameter will be larger than that following from the 1D–2T–HD simulation neglecting the lateral heat transfer. It is important that the separation takes place during the temporal range of the order of the acoustic time scale $t_s = d_f/c_s$ (few tens of picoseconds) [5,15]. 2T stage in gold lasts approximately 10 ps. Of course, cooling continues at the 1T stage. But such cooling is slow, it continues much longer than t_s , and therefore it cannot influence the separation diameter.

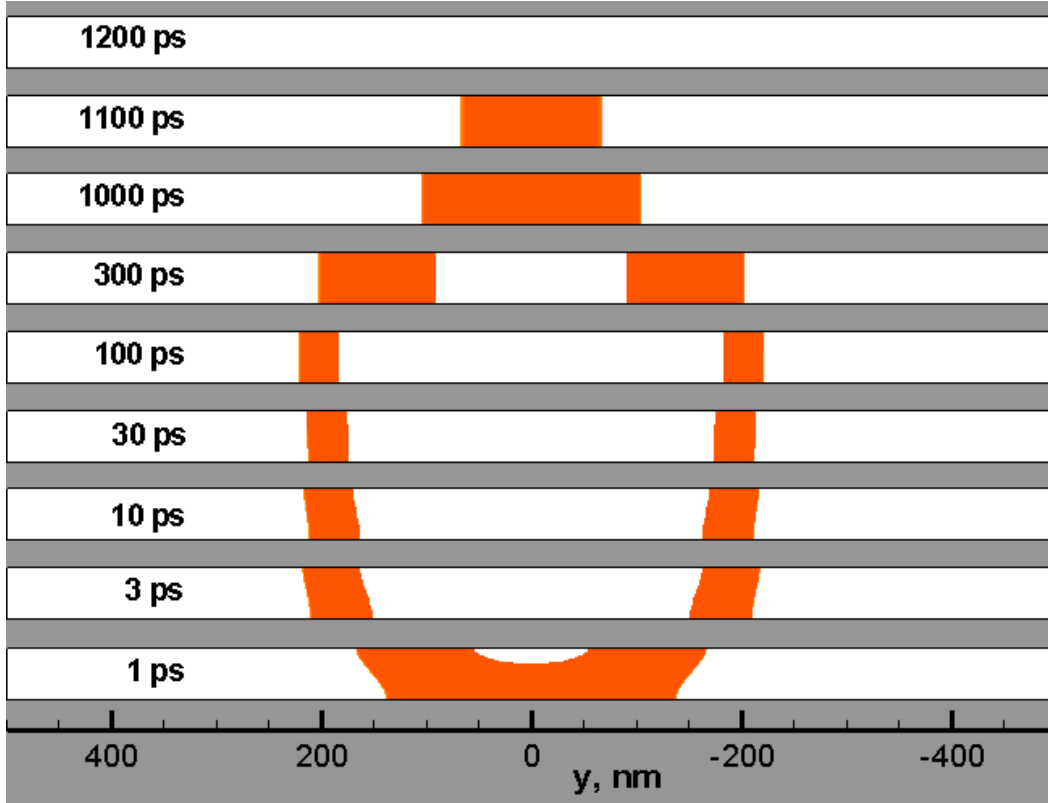


Figure 4. Evolution of the melting zone is shown. The melting zone (the orange strips) is filled with solid–liquid mixture. Pure liquid is inside the zone, while the pure solid is outside. The zone (i) appears, (ii) quickly lose dependence on film thickness (see the frame for the instant $t = 1$ ps), and (iii) after that spread laterally. The zone achieves its maximum extension at $t \approx 100$ ps—significantly later than the separation takes place. But expansion of the zone is small during the temporal interval between the instant of separation of a film from substrate $t = 20$ – 30 ps and the instant when the maximum expansion of melting is achieved. At the final stage expansion of melting is changed to contraction of the liquid spot thanks to recrystallization. The hot spot cools down and totally solidifies at nanosecond time scale for chosen size $2R_L = 360$ nm and amount of energy 50 mJ/cm^2 .

The effect from fast 2T lateral flux is stronger if the beam is more narrow. Therefore we take the value $2R_L = 360$ nm for simulation below. This seems corresponds to the strongest achievable optical focusing today. In bulk gold, the HAZ has thickness $d_T = 100$ – 200 nm. This is the upper limit for the 2T lateral heat propagation.

Simulations show that even for $2R_L = 360$ nm the lateral enlargement of the energy distribution along the axis y during the stage lasting few tens of picoseconds is small. For the problem (I) there is small difference between the plane calculation (cylindrical lens, distribution in plane x – y) from one side and the axisymmetric calculation (coordinates are: cylindrical axis z and cylindrical radius r_{cyl}) from the other side. This is because the time is short and lateral heat propagation during this time interval is small relative to R_L .

(II) Second, we want to simulate the freezing process at the late stage quantitatively, avoiding the analytical estimates. To freeze the molten hot spot we have to expand the absorbed energy over the area larger than the area covered by the circle R_L (energy conservation). In this

case geometry (plane or axisymmetric) is significant. In plane geometry (cylindrical lens) the divergence of the heat flux is smaller. Then freezing time is longer. The melting–freezing process is shown in figure 4.

In our simulation when thermal processes run in isochoric regime the melting zone has finite thickness. This corresponds to finite width (along the straight $\rho = \text{const}$) of a melting strip on the phase diagram at the ρ – T plane of the EoS [11, 12, 22–26]. Melting begins at the outside boundaries of the orange strips in figure 4. This corresponds to intersection of solidus; solidus and liquidus bound the melting strip at the ρ – T plane. The liquid–solid mixture finishes transferring into pure liquid at the inner boundaries (this is liquidus) of the orange strips in figure 4.

System of equations (1) and (2) is solved with equilibrium EoS. As was said, finite thickness of the melting zone (orange strips) in figure 4 follows from finite thickness of the melting strip at the ρ – T plane. Comparison of simulations done with 2T hydrodynamic code with equilibrium EoS and molecular dynamics (MD) simulations is given in [27]. MD code is free from constraints to be equilibrium. Melting zone in MD is very wide at the 2T stage. Initially it is composed totally from liquid–solid mixture. Thus it is similar to the case shown in the bottom frame in figure 4 corresponding to the instant $t = 1$ ps. Also at the recrystallization stage the mixture zone in MD is wide as it is in figure 4 at the stage $t \approx 1$ ns. Comparing 2T hydrodynamics and MD according to [27] we can conclude that they agree rather well with each other.

5. Conclusion

For the first time, the 2T–2D approach is used to describe the edge effects of thermal transfer from a solitary hot spot created by a femtosecond action onto a thin film. We consider thermal transfer accompanied by first order phase transition (melting and solidification). Heat of fusion is accurately included into simulation, while usually people solving 2T equations say about melting or recrystallization only relating to the melting temperature.

It is shown that the expansion of heat out of the laser spot at the 2T stage and prior to the delamination stage is small even for spot diameter near 400 nm. At larger diameters the effects from 2T heat expansion becomes negligible. Presented simulations allow following the process that leads to total solidification. The solidification is important as it stops motion of bumps and keep their shapes for postmortem analysis [1–7].

Acknowledgments

Authors have been supported by Russian Foundation for Basic Research grant No. 16-08-01181.

References

- [1] Korte F, Koch J and Chichkov B N 2004 *Appl. Phys. A* **79** 879–81
- [2] Unger C, Koch J, Overmeyer L and Chichkov B N 2012 *Opt. Express* **20** 24864
- [3] Ivanov D S, Kuznetsov A I, Lipp V P, Rethfeld B, Chichkov B N, Garcia M E and Schulz W 2013 *Appl. Phys. A* **111** 675–87
- [4] Nakata Y, Miyanaga N, Momoo K and Hiromoto T 2013 *Appl. Surf. Sci.* **274** 27–32
- [5] Inogamov N A, Zhakhovsky V V, Khokhlov V A, Kuchmizhak A A and Kudryashov S I 2016 *J. Phys.: Conf. Ser.* **774** 012102
- [6] Kuchmizhak A *et al* 2016 *Nanoscale* **8** 12352–61
- [7] Inogamov N A, Zhakhovsky V V, Khokhlov V A, Petrov Yu V and Migdal K P 2016 *Nanoscale Res. Lett.* **11** 177
- [8] Pohl R *et al* 2015 *Phys. Rev. Appl.* **3** 024001
- [9] Schrider K J, Torralva B and Yalisove S M 2015 *Appl. Phys. Lett.* **107** 124101
- [10] Lorenz P, Ehrhardt M and Zimmer K 2014 *Phys. Procedia* **56** 1015–23
- [11] Povarnitsyn M E, Itina T E, Sentis M, Khishchenko K V and Levashov P R 2007 *Phys. Rev. B* **75** 235414
- [12] Povarnitsyn M E, Itina T E, Levashov P R and Khishchenko K V 2013 *Phys. Chem. Chem. Phys.* **15** 3108–14
- [13] Povarnitsyn M E and Itina T E 2014 *Appl. Phys. A* **117** 175–8

- [14] Khokhlov V A, Zhakhovsky V V, Khishchenko K V, Inogamov N A and Anisimov S I 2016 *J. Phys.: Conf. Ser.* **774** 012100
- [15] Inogamov N A and Zhakhovsky V V 2016 *J. Phys.: Conf. Ser.* **681** 012001
- [16] Anisimov S I, Kapeliovich B L and Perel'man T L 1974 *Sov. Phys. JETP* **39** 375–7
- [17] Gurevich E L, Levy Y, Gurevich S V and Bulgakova N M 2017 *Phys. Rev. B* **95** 054305
- [18] Petrov Yu V, Inogamov N A and Migdal K P 2013 *JETP Lett.* **97** 20–7
- [19] Migdal K P, Petrov Yu V and Inogamov N A 2013 *Proc. SPIE* **9065** 906503
- [20] Petrov Yu V, Migdal K P, Inogamov N A and Anisimov S I 2016 *JETP Lett.* **104** 431–9
- [21] Migdal K P, Petrov Yu V, Il'nitsky D K, Zhakhovsky V V, Inogamov N A, Khishchenko K V, Knyazev D V and Levashov P R 2016 *Appl. Phys. A* **122** 408
- [22] Khishchenko K V, Tkachenko S I, Levashov P R, Lomonosov I V and Vorobev V S 2002 *Int. J. Thermophys.* **23** 1359–67
- [23] Levashov P R, Khishchenko K V, Lomonosov I V and Fortov V E 2004 *AIP Conf. Proc.* **706** 87–90
- [24] Khishchenko K V 2008 *J. Phys.: Conf. Ser.* **98** 032023
- [25] Inogamov N A *et al* 2012 *AIP Conf. Proc.* **1464** 593–608
- [26] Petrov Yu V, Migdal K P, Inogamov N A and Zhakhovsky V V 2015 *Appl. Phys. B* **119** 401–11
- [27] Inogamov N A, Zhakhovskii V V, Ashitkov S I, Khokhlov V A, Petrov Y V, Komarov P S, Agranat M B, Anisimov S I and Nishihara K 2009 *Appl. Surf. Sci.* **255** 9712–6